IEEE Access
Multidisciplinary | Rapid Review | Open Access Journal

Received 21 January 2023, accepted 2 February 2023, date of publication 6 February 2023, date of current version 23 February 2023.

Digital Object Identifier 10.1109/ACCESS.2023.3242975

RESEARCH ARTICLE

Simulation of Stray and Core Shielding Loss for Power Transformer Based on 2D/3D FEM

WEN-CHING CHANG[1], (Member, IEEE), CHENG-CHIEN KUO[1], WEN-CHENG LIN[2], AND MIN-NAN HSIEH[2], (Member, IEEE)

[1]Department of Electrical Engineering, National Taiwan University of Science and Technology, Taipei 106, Taiwan
[2]Shihlin Electric, Hsinchu 303, Taiwan

Corresponding author: Cheng-Chien Kuo (cckuo@mail.ntust.edu.tw)

ABSTRACT In recent years, the capacity has increased and the volume has been limited in the power transformers. The stray losses of the tanks and structural parts cannot be ignored in the load loss. The tanks and the structural parts are complex structures. It is difficult for transformer manufacturers to use analytical methods to calculate stray losses for each component in the power transformers. If the stray loss distribution of the components can be estimated, it will help to optimize the power transformer's cost and performance. Therefore, this paper uses the finite element method to solve the stray loss of components in the time-varying magnetic field. At the same time, the core losses of the magnetic shielding are solved. In addition, the position of the tap is considered, and the proposed stray loss model has the temperature factor, which can improve the accuracy of the simulation results. Finally, the short circuit test experiment is carried out in the 350 MVA three-phase five-limb power transformer. The proposed models and material parameters are verified by the experimental results.

INDEX TERMS Finite element analysis, power transformer, stray loss, impedance boundary.

I. INTRODUCTION

In recent years, the design of transformers has been limited by size due to the application field and transportation of transformers [1]. When the size of the transformer is decreased, the cost and performance are affected in the transformer. According to the European Union Commission Regulation No. 548/2014, the distribution transformer and power transformer must conform to the framework of ecological design, which achieves energy saving and reduces carbon dioxide emissions. The tier 1 level and tier 2 level standards have been proposed in the power transformer. Currently, the power transformer is necessary to meet the peak efficiency index of tier 2 level standard. The factors of peak efficiency index include open circuit loss, short circuit loss, the electrical power of the cooling system and rate power in the power transformer [2], [3]. In [4], the results show that when the distribution transformer design adopts the tier 2 standard, the initial total cost of ownership is relatively high due to the low price of electric energy. With the increase of time and load, the design adopts the tier 2 standard is more economical than the design adopts the tier 1 and DIN42500 standards. In [5], the energy consumption of the transformer and the daily price of electricity are considered, the results show the low-efficiency transformers only have advantages in initial investment, and will increase energy costs in long-term operation. Therefore, it is more economical to adopt and manufacture transformers with higher efficiency when the energy price becomes higher and the load increases. However, transformer manufacturers need to strike a balance between cost and performance. The cost factors include material cost, labor cost, and indirect cost [6], [7]. The performance of the power transformer needs to meet the technical specification standards, such as short circuit impedance. At the same time, the equipment needs to have a good life cycle and efficiency. The life cycle and efficiency depend on losses in the transformer. The losses of power transformers are composed of two major losses: open circuit loss and short circuit loss. The open circuit loss is caused by the iron core. The short circuit loss is composed of copper loss and stray

The associate editor coordinating the review of this manuscript and approving it for publication was Amin Mahmoudi.

loss. The copper loss is caused by the windings, which means the current flows through DC resistance in the windings. The stray loss is caused by the high magnetic permeability and high conductivity of the components, such as tanks, structural parts, and windings. Therefore, with the power transformer's capacity increase and volume limit, the proportion of stray losses caused by the tank and structural parts cannot be ignored. This has led transformer manufacturers to add magnetic shielding to reduce stray losses.

However, magnetic shielding is added too much or misplaced, resulting in increased cost and reduced performance. If the stray loss distribution of the power transformer can be solved, the magnetic shield's optimal design can balance cost and performance. In recent years, many scholars have used the finite element method to analyze and study the characteristics of power transformers. The finite element models determine the accuracy of the results. In [8], the tank of stainless steel mixed with low-carbon steel material has especially been considered in the bushing finite element modes. The stray loss results show that the proposed 2D axisymmetric model has certain feasibility. In [9], the heat conduction coefficient has been considered in ascending flange finite element models, and the stray loss distribution is solved in the magnetic-thermal coupling field. In [10], the harmonic factor and DC bias factor have been considered in the transformer finite element models, and the design of the lobe-type magnetic shielding was optimized according to the simulation results. In [11] and [12], the skin effect meshing method and impedance boundary method are compared based on the 3D transformer finite element model, the results show that the calculation time was shortened by 4 times by using the impedance boundary method. In [13] and [14] the temperature factor of the core and the structural factor of the magnetic shielding have been considered in the 3D finite element models, which are verified by the temperature field.

According to the above applications, it is understood that the finite element models include 3D geometrical models, material factors, boundary conditions, and field selection. Also, it is shown that impedance boundary condition is beneficial for complex geometries to solve stray loss distribution. Therefore, this paper proposed three-phase five-limb transformer finite element models, which solve stray loss distribution. The geometrical models are composed of the core, HV/LV/Tap windings, structural parts, magnetic shielding, and tank. Due to the influence of the eddy current in the components, the time-varying magnetic field is chosen. In addition, the position of the winding taps operates differently, resulting in a different stray loss distribution, so the position of the windings taps must be considered. The temperature factors are specially added to the impedance boundary condition, which affects the accuracy of the stray loss distribution. Next, this paper is divided into four sections; each section is summarized: Section II introduces the finite element analysis model, which includes Maxwell solver equations, leakage inductance model, stray loss model, and magnetic shielding core loss model. Section III shows finite element simulation results, which include 2D simulation results and 3D simulation results. The 2D simulation results are to solve the position of the winding taps. The 3D simulation results are to solve components' stray loss distribution. Section IV shows 350 MVA three-phase five-limb experimental results, which verify the proposed 2D/ 3D finite element models. Section V describes the conclusion of this paper.

II. FINITE ELEMENT ANALYSIS MODELS

A. MAXWELL SOLVER EQUATIONS

Maxwell solver equations are divided into four equations: Ampere's law, Faraday's law, Gauss's law of magnetism, and Gauss's law. Differential forms of Maxwell solver equations can be written as:

$$\text{Ampere's law} : \nabla \times H = J + \frac{\partial D}{\partial t} \tag{1}$$

$$\text{Faraday's law} : \nabla \times E = -\frac{\partial B}{\partial t} \tag{2}$$

$$\text{Gauss's law for magnetism} : \nabla \cdot B = 0 \tag{3}$$

$$\text{Gauss's law} : \nabla \cdot D = \rho \tag{4}$$

In the (1)-(4), the symbol H is the magnetic field intensity (A/m), the symbol J is conduction current density (A/m^2), the symbol D is the electric displacement (C/m^2), the symbol E is the electric field (V/m), the symbol B is the magnetic flux density (T), and the symbol ρ is the charge density (C/m^2). Due to the operating frequency of the power transformer being 60 Hz, the displacement current is ignored.

B. LEAKAGE INDUCTANCE MODEL

In general, the tap windings of the step-down power transformers are designed to adjust the high-side voltage. However, the leakage inductance is affected by the operating positions of the tap winding, and the leakage inductance is related to the stray loss in the components. Therefore, the leakage inductance must be solved before the stray loss distribution is solved, and the leakage inductance considers the tap winding position.

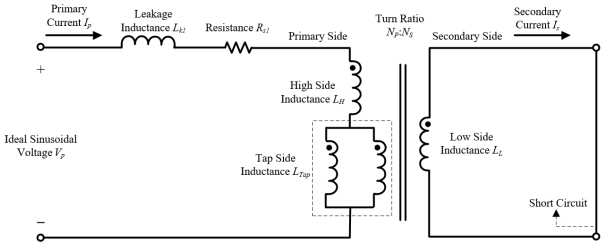

FIGURE 1. The short circuit of the power transformer diagram.

The equivalent short circuit diagram is shown in Fig. 1, which is composed of the ideal sinusoidal voltage V_p, equivalent leakage inductance L_{k1}, equivalent resistance R_{s1}, high side inductance L_H, tap side inductance L_{Tap}, and low side inductance L_L. The tap windings are composed of the same two windings in parallel connection.

To simplify the analysis, some conditions are assumed as follows:

1) The ideal sinusoidal voltage V_p is the ideal voltage source and is balanced in each phase;
2) The primary current I_p and secondary current I_s are ideal sine waves;
3) The secondary side output terminal is shorted;
4) The magnetizing reactance and parallel resistance are neglected, and the excitation current is neglected;
5) The turns ratio is primary side total turns to secondary side turns, which is defined as $N = N_P/N_S$;

Due to the magnetic flux generated by the windings, the magnetic flux is not fully conducted and is stored in the form of energy. The primary current I_p is an ideal sine wave, the equation of the instantaneous energy can be written as:

$$W_{Instant} = \frac{1}{2}L_{k1}[I_{p,peak}Cos(\omega t + \theta)]^2 \tag{5}$$

In (5), the symbol $I_{p,peak}$ is the peak current on the primary side, and the symbol θ is the initial angle of the primary current. If the initial angel is zero, and the equation of instantaneous energy takes the average under the period, which can be written as:

$$W_{Average} = \frac{1}{2\pi}\int_0^{2\pi} W_{Instant}\, d\omega t = \frac{1}{4}\int_v B \cdot H^* dv \tag{6}$$

In (6), the symbol B is the magnetic flux density, and the symbol H^* is the complex conjugate of the magnetic field intensity. According to (6), the primary side equivalent leakage inductance L_{k1} can be obtained:

$$L_{k1} = \frac{\int_v B \cdot H^* dv}{I_{p,peak}^2} = \frac{4W_{Average}}{I_{p,peak}^2} \tag{7}$$

The equation of per unit impedance can be written as:

$$Z_{pu} = \frac{Z}{Z_B} \tag{8}$$

In (8), the symbol Z and the symbol Z_B are defined as:

$$\text{Impedance} : Z = R_{s1} + XL_{k1} = R_{s1} + 2\pi f L_{k1} \tag{9}$$

$$\text{Impedance Base} : Z_B = \frac{S_B}{3I_p^2} \tag{10}$$

Assumed that the equivalent leakage reactance L_{k1} is bigger than the equivalent series resistance R_{s1} on the primary side. The equivalent series resistance is ignored, and (7)-(10) are combined to obtain:

$$Z_{pu} = \frac{X_{Lk1}}{Z_B} = \frac{6I_p^2\pi f \int_v B \cdot H^* dv}{S_B I_{p,peak}^2} \tag{11}$$

C. STRAY LOSS MODEL

The skin depth must be considered in the components, due to the eddy current value is related to the component thickness. In the 3D geometric model's traditional solution, it is needed to make fine mesh cutting, the computer hardware is often unable to support a large number of mesh. Therefore, the 3D geometric model is advantageously solved using impedance boundary conditions, which only require mesh cutting on the surface of the component. At present, the impedance boundary conditions didn't add the temperature factor, which cannot reflect the actual material state in the conductor components. Next, the impedance boundary condition with temperature factor is introduced.

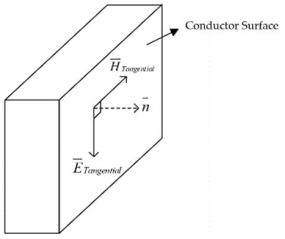

FIGURE 2. The relationship of electric field and magnetic field intensity at the conductor surface.

At the conductor surface, there is a relationship between the tangential electric field and the tangential magnetic field strength [15], and as shown in Fig. 2. The equation can be written as:

$$\vec{E}_{Tangential} = Z_s(\vec{H}_{Tangential} \times \vec{n}) \tag{12}$$

In (12), the symbol $\vec{E}_{Tangential}$ is the tangential electric field, the symbol $\vec{H}_{Tangential}$ is the tangential magnetic field strength, the symbol $\vec{n}$ is the unit vector, the symbol Z_s is the surface impedance. In (12), the surface impedance is defined:

$$Z_s = (1+j)\sqrt{\frac{\omega\mu}{2\sigma}} = \frac{(1+j)\omega\mu\delta}{2} \tag{13}$$

In (13), the symbol μ is the magnetism of relative permeability, the symbol σ is the conductivity, the symbol δ is the skin effect. The poynting vector takes the average under the period to obtain the complex poynting vector density, which can be written as:

$$S_{poynting} = \frac{1}{2}\text{Re}(\vec{E} \times \vec{H}^*) \tag{14}$$

In (14), the symbol $\vec{E}$ is the electric field, and the symbol $\vec{H}^*$ is the complex conjugate of the magnetic field intensity. Assuming that the surface is only considered in (14), and combination of (12) and (14) can be obtained:

$$S_{Poynting,Surface} = \sqrt{\frac{\omega\mu}{8\sigma}}(\vec{H}_{Tangential}\vec{H}^*_{Tangential}) \tag{15}$$

Equation (15) takes surface integral, which is the total loss at the surface, and can be written as:

$$S_{StrayLoss} = \sqrt{\frac{\omega\mu}{8\sigma}}\int_{Surface}(\vec{H}_{Tangential}\vec{H}^*_{Tangential})ds \tag{16}$$

The conductivity temperature coefficient is defined as:

$$\sigma = \frac{\sigma_{20}}{[1+\alpha_{20}(t-20)]} \tag{17}$$

In (17), The symbol σ_{20} is the conductivity at 20 °C, the symbol α_{20} is the temperature coefficient at 20 °C, and the

symbol t is the temperature. Combing (16) and (17), the total loss is considered conductivity temperature coefficient, which can be written as:

$$S_{Temp} = \sqrt{\frac{\omega\mu[1+\alpha_{20}(t-20)]}{8\sigma_{20}}} \int_{Surface} (\vec{H}_{Tangential}\vec{H}^{*}_{Tangential})ds \tag{18}$$

D. MAGNETIC SHIELDING CORE LOSS MODEL

Power transformers add magnetic shielding to reduce eddy current losses, but the magnetic shielding cores also create losses, including hysteresis losses, eddy current losses, and extra losses [16]. The magnetic shielding core loss can be written as:

$$P_v = P_h + P_c + P_e \tag{19}$$

In (19), The symbol P_h is the hysteresis loss, the symbol P_c is the eddy current loss, and the symbol P_e is the extra loss. Many factors are considered in the model, the factors include conductivity, thickness, mass density, nonlinear *P-B* and nonlinear *P-H* curves, and operating frequency. According to the above factors, hysteresis loss, eddy current loss, and extra loss are defined as:

$$P_h = k_h f_0 B_m^2 \tag{20}$$
$$P_c = k_c (f_0 B_m)^2 \tag{21}$$
$$P_e = k_e (f_0 B_m)^{1.5} \tag{22}$$

In (20)-(22), the symbol k_h is the hysteresis loss coefficient, the symbol k_c is the eddy current loss coefficient, the symbol k_e is the extra loss coefficient, and the symbol B_m is the magnetic flux density of magnetic shielding, and the symbol f_0 is the operating frequency.

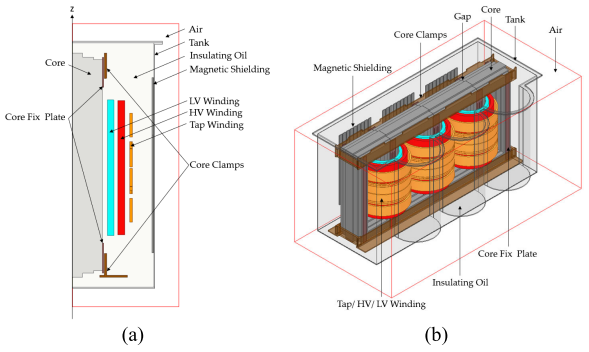

FIGURE 3. Simulation model diagram. (a) 2D axisymmetric model. (b) 3D model.

III. FINITE ELEMENT ANALYSIS SIMULATION

A. POWER TRANSFORMER SIMULATION MODEL

There are two types of three-phase five-limb simulation models, which are 2D axisymmetric models and 3D models, and shown in Fig.3. The simulation models are composed of windings, core, insulating oil, structural parts, and magnetic shielding. The winding can be divided into low voltage side winding, high voltage side winding, and tap winding. The tap windings are divided into two coils, which are connected in parallel. The structural parts are divided into core fix plate and core clamp. The z-axis is defined as the axisymmetric axis of the 2D axisymmetric model. The gaps of the core are considered in the 3D model. The full-length slots are considered in the inner core fix plate. The core is equivalent to the three-layer type. To focus on the large block in the model, the hole is ignored in all components of models. The winding model is equivalent to the cylinder geometry, and the oil channel is ignored. The bushing is ignored in the tank.

TABLE 1. Material parameter of simulation model.

Name	Material	Parameter
Winding	Copper	Resistivity = 1.68×10^{-8} Ω·m Magnetism of Relative Permeability = 1
Iron Core	Electrical Grade Sheet	Conductivity = 2083300 S/m Mass Density = 7650 kg/m^3 Magnetism of Relative Permeability = Non-linear *B-H* Curve
Magnetic Shielding	Electrical Grade Sheet	Conductivity = 2173900 S/m Mass Density = 7650 kg/m^3 Magnetism of Relative Permeability = Non-linear *B-H* Curve
Structural Parts, Tank	Carbon Steel	Conductivity = 6029411 S/m @ 20 °C Magnetic of Relative Permeability = 200 Temperature Coefficient = 0.005
Insulating Oil, Gap	Oil	Magnetism of Relative Permeability: 1
Environment	Air	Magnetism of Relative Permeability: 1.0000004

The material parameters of the simulation model are shown in Table 1. The simulated material factors, including electrical conductivity, magnetism of relative permeability and mass density. In addition, the temperature factor is considered in the structural parts and tank, the temperature coefficient is defined as 0.005.

The magnetism of relative permeability is the non-linear curve in the iron core and magnetic shielding, and the *B-H* curves are shown in Fig. 4. The *P-B* curve is a non-linear curve in the magnetic shielding, and the curve is shown in Fig. 5.

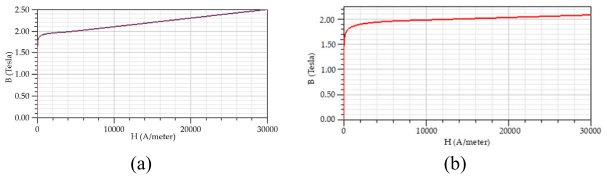

FIGURE 4. The B-H curve of electrical grade sheet diagram. (a) Iron Core. (b) Magnetic Shielding.

The eddy current loss model is the classic model, which is considered conductivity, thickness of the magnetic shielding. At the same time, according to the material and *P-B* curve in the magnetic shielding, the loss coefficients can be solved by the least square method [16]. When the magnetic shielding operates at 60 Hz, the loss coefficients of magnetic shielding

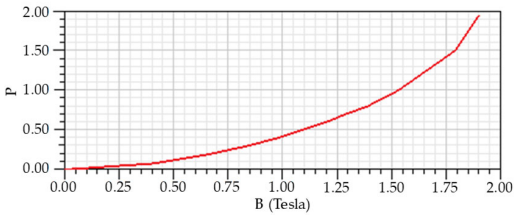

FIGURE 5. The P-B curve of the magnetic shielding diagram.

are shown in Table 2. The coefficient of hysteresis loss k_h is 0.00833294 W/kg, and the coefficient of eddy current loss k_c is 4.20697×10^{-5} W/kg. The coefficient of extra loss k_e is 0 W/kg.

TABLE 2. Loss coefficients of magnetic shielding (@60 HZ).

Name	Parameter
Coefficient of Hysteresis Loss k_h	0.00833294 W/kg
Coefficient of Eddy Current Loss k_c	4.20697×10^{-5} W/kg
Coefficient of Extra Loss k_e	0 W/kg

TABLE 3. Specification of power transformer.

Name	Parameter
Capacity	350 MVA
Primary Voltage	177.1/ 161/ 144.9 kV
Secondary Voltage	66 kV

B. WINDING EXCITATION PARAMETERS

The specification table of the power transformer is shown in Table 3. The Capacity is 350 MVA, the rated voltage of the primary side is 161 kV, and the rated voltage of the secondary side is 66 kV. The adjustment range is 10 % in the primary side voltage, which means the maximum voltage is 177.1 kV and the minimum voltage is 144.9 kV.

TABLE 4. Parameters of winding excitation.

	Name	Parameter
Maximum Tap Condition	High Side Winding	658.59 A/ 478 Turn
	Tap Side Winding	329.295 A/ 262 Turn
	Low Side Winding	3061.69 A/ 131 Turn
Rated Tap Condition	High Side Winding	725.28 A/ 478 Turn
	Tap Side Winding	362.64 A/ 150 Turn
	Low Side Winding	3061.69 A/ 131 Turn
Minimum Tap Condition	High Side Winding	805.38 A/ 478 Turn
	Tap Side Winding	402.69 A/ 40 Turn
	Low Side Winding	3061.69 A/ 131 Turn

The connection method of the primary side is the Delta connection, and the connection method of the secondary side is the Start connection. According to the capacity and connection method, the excitation parameters of the windings are shown in Table 4. The primary side windings include the high voltage side winding and the tap winding. The secondary side winding is the low voltage side winding. The tap windings are divided into two coils for parallel connection, and the tap winding current is half of the primary winding current. The primary side voltage is 177.1 kV as the maximum tap condition. The primary side voltage is 166.1 kV as the rated tap condition. The primary side voltage is 144.9 kV as the minimum tap condition.

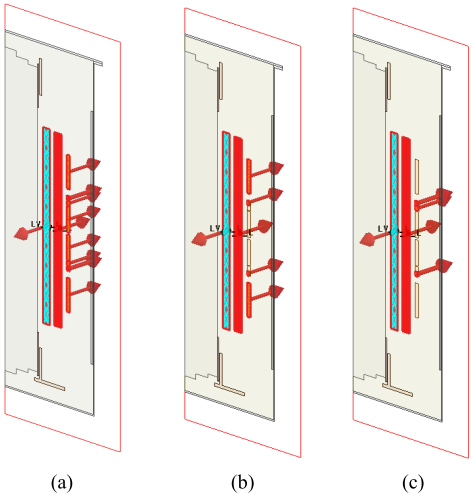

FIGURE 6. Windings excitation and direction in the axisymmetric 2D model. (a) Max Condition. (b) Rated Condition. (c) Min Condition.

The excitation positions of the tap winding are shown in Fig. 6. It is defined that the current direction of the primary side winding is opposite to the current direction of the secondary side. In the maximum tap condition, all the tap windings are excited. In the rated tap condition and minimum tap condition, some of the tap coils are not excited.

C. SIMULATION RESULTS

In this chapter, the stray loss distributions of three-phase five-limb power transformers are analyzed based on the proposed simulation models and the proposed finite element analysis models. First, the three conditions are analyzed in the axisymmetric 2D finite element model, which is the leakage inductance model, and the condition with severe leakage inductance can be obtained in the simulation results. Finally, the stray loss distribution and maximum total loss are analyzed by the proposed 3D finite element models, which are the stray loss model and the magnetic shielding core loss model.

TABLE 5. Simulation results of per unit impedance.

Name	$W_{average}$ (J)	L_{kl} (H)	X_{Lk} (Ohm)	Z_{PU} (%)
Max Condition	27197	0.12540	47.253	17.56
Rated Condition	25908	0.09850	37.116	16.73
Min Condition	24571	0.07576	28.547	15.87

The simulation results of the energy distribution diagrams are shown in Fig. 7. In the three conditions, the energy is distributed between the low voltage winding and the high

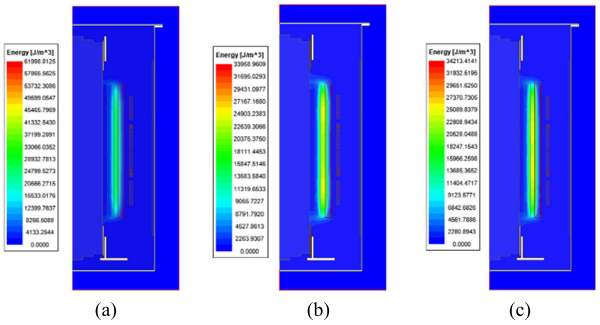

FIGURE 7. Simulation results of energy distribution in the axisymmetric 2D model. (a) Max Condition. (b) Rated Condition. (c) Min Condition.

voltage winding, which means the leakage fluxes of the windings are concentrated in the regions with low magnetism of relative permeability. According to the proposed leakage inductance model, the per unit impedances of simulation results are shown in Table 5. The average energy is 27197 J, and per unit impedance is 17.56 % in the maximum tap condition. The average energy is 25908 J, and per unit impedance is 16.73 % in the rated tap condition. The average energy is 24571 J, and per unit impedance is 15.87 % in the minimum tap condition. According to the above axisymmetric 2D model of simulation results, the average energy in the maximum tap condition is the largest, which means that the magnetic flux leakage phenomenon of winding is the most serious. Continuing, the maximum tap condition is simulated in the 3D mode.

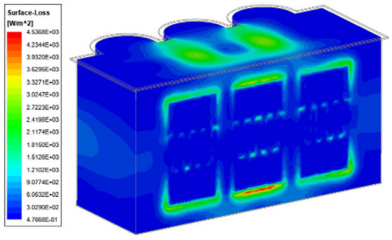

FIGURE 8. Stray loss distribution of simulations results at back direction.

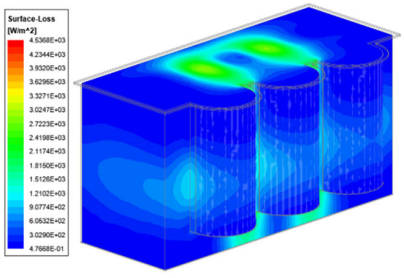

FIGURE 9. Stray loss distribution of simulations results at front direction.

The stray loss of simulation result in the tank is shown in Fig. 8, Fig. 9 and Fig. 10. The simulation results show that the stray loss distribution is concentrated on the tank above and below the junction between the windings, and the stray loss distribution is concentrated around the magnetic shielding and seam of the magnetic shielding.

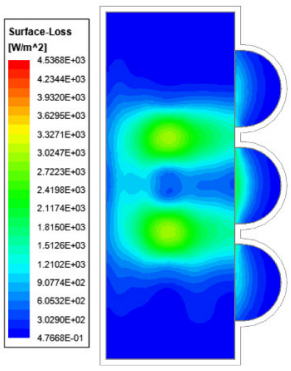

FIGURE 10. Stray loss distribution of simulations results at bottom direction.

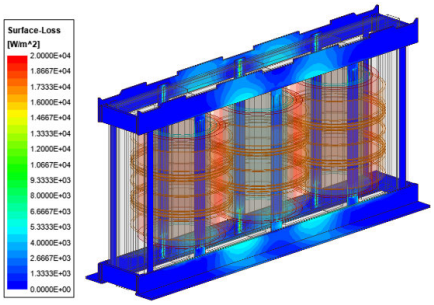

FIGURE 11. Stray loss distribution of simulation results in the structural parts.

The stray loss of simulation results in the structural parts shown in Fig. 11. The stray loss distribution is concentrated above and below the core fix plate, and the stray loss of the outer core fix plate is lower. The stray loss distribution is concentrated in the middle of the core clamp, which is above and below the junction between the winding.

The core loss of simulation results in the magnetic shielding is shown in Fig. 12. The core loss is concentrated middle in the magnetic shielding.

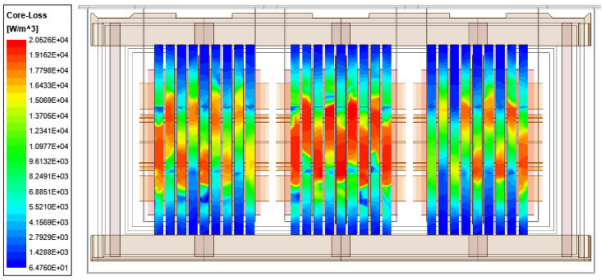

FIGURE 12. Core loss distribution of simulation results in the magnetic shielding.

The simulation results data about stray loss and magnetic shielding loss are shown in Table 6. The simulated total loss is 120845 W, in which the percentage of the core fix plate loss is 11.20 %, the percentage of the core clamp loss is 36.50 %, and the percentage of tank loss is 51.04 %, the percentage of magnetic shielding loss is 1.26 %. stray loss and core loss.

The above simulation results are the temperature of structural material at 20 °C.

TABLE 6. Simulation results stray loss and magnetic shielding loss.

Name	Core Fix Plate	Core Clamp	Tank	Magnetic Shielding	Total
Loss (W)	13524	44114	61682	1525	120845
Percentage (%)	11.20	36.50	51.04	1.26	100

According to the (18) and temperature coefficient in Table 1, the temperature factor is considered in the stray loss. The simulation results of the tank and structural parts under different temperatures are shown in Fig. 13. When the temperature parameter is higher, the stray losses of the tank and structural parts are higher.

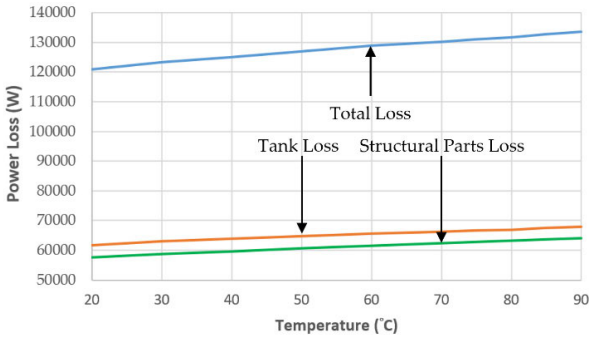

FIGURE 13. The simulation results of tank loss and structural parts loss under different temperatures.

IV. EXPERIMENTAL RESULTS

The proposed finite element model of eddy currents is validated by the experimental results of short circuit tests in this section. First, the 350 MVA power transformer is subjected to short circuit test experiments, which measured the actual data. The actual data includes per unit impedance and load loss. The measured per unit impedance as shown in Table 7. In the maximum tap condition, the measured per unit impedance is 18.31 %, and the error is 4.10 %. In the rated tap condition, the measured per unit impedance is 17.37 %, and the error is 3.68 %. In the minimum tap condition, the measure per unit impedance is 16.31 %, and the error is 2.70 %.

TABLE 7. Experimental results of per unit impedance.

Name	Max Tap Condition		Rated Tap Condition		Min Tap Condition	
	Measured Results	Simulation Results	Measured Results	Simulation Results	Measured Results	Simulation Results
Z_{pu} (%)	18.31	17.56	17.37	16.73	16.31	15.87
Error (%)	4.10 %		3.68 %		2.70	

The measured load losses are composed of winding losses, structural stray losses, tank stray losses, and magnetic shielding core losses. The measured stray loss is defined as not considered the winding loss. The measured stray loss of the power transformer under maximum condition as shown in Table 8. The stray loss of experimental result is 131654 W. According to the proposed equations, when temperature is 20 °C, 40 °C, 60 °C and 80 °C, the simulation error is 8.21%, 5.02%, 2.20%, 0.03 %.

TABLE 8. Experimental results stray loss and shielding loss.

Name	Max Tap Condition				
	Measured Results	Simulation Results			
		20 °C	40 °C	60 °C	80 °C
Core Fix Plate Loss (W)	-	13524	13852	14172	14480
Core Clamp Loss (W)	-	44114	45837	47410	48672
Tank Loss (W)	-	61682	63827	65645	66923
Shielding Loss (W)	-	1525	1528	1529	1532
Total Loss (W)	131654	120845	125044	128756	131607
Error (%)	0	8.21	5.02	2.20	0.03

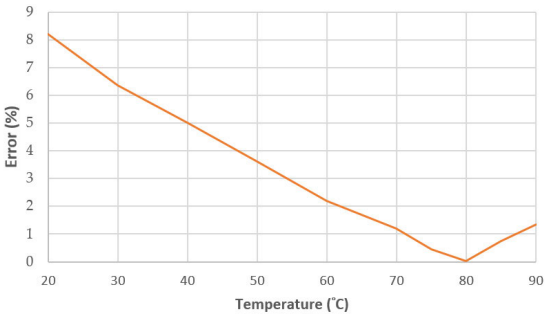

FIGURE 14. The simulation results of error under different temperatures.

The measured temperature of insulating oil is about 61 °C in the short circuit test experiment. In fact, the components with energy consumption are the source of the temperature, which is higher than the temperature value of insulating oil. The simulation results of the error as shown in Fig. 14. According to the simulation results, the error is lowest at temperatures 80 °C.

V. CONCLUSION

In this paper, the stray loss of power transformer is simulated based on finite element method, and the simulation results are verified by the short circuit experimental results of 350 MVA power transformer. The proposed finite element analysis model includes the leakage inductance reactance model, stray loss model and magnetic shielding core loss model. The nonlinear magnetic material factor, mass density, thickness and operating frequency are considered in the magnetic shielding core loss model. The stray loss model adopts the surface impedance method, which has the advantage of fast calculation speed. It has considerable advantages for complex structural parts and tank in the 3D models. In addition, this

paper also considers the temperature coefficient in the surface impedance method, which makes the simulation results more accurate. Moreover, through the 2D axisymmetric finite element analysis model, the influence of the tap condition can be quickly obtained from the leakage inductance. According to the 3D finite element analysis model, the stray loss distribution is on the tank above and below the junction between the windings, and the stray loss distribution in the core clamp is also having the same trend. Based on the simulation results and experimental results, the minimum error per unit impedance is 2.70 %. The minimum error total stray loss is 0.03 % under 80 °C. Finally, according to the proposed finite element analysis model, the stray loss distribution is accurately predicted in the structural parts and tank. It is helpful for transformer manufacturers to understand the loss ratio and loss distribution in the structural parts and tank, which optimizes the design of the magnetic shielding core, and improve the efficiency and reliability of the three-phase five-limb transformer.

APPENDIX

Appreciate Shihlin Electric for supporting this research.

REFERENCES

[1] G. Jose and R. Chacko, "A review on wind turbine transformers," in *Proc. Annu. Int. Conf. Emerg. Res. Areas, Magn., Mach. Drives (AICERA/iCMMD)*, Jul. 2014, pp. 1–7.

[2] *Implementing Directive 2009/125/EC of the European Parliament and of the Council With Regard to Small, Medium and Large Power Transformers*, document 548/2014, Commission Regulation (EU), May 2014. [Online]. Available: https://eur-lex.europa.eu/eli/reg/2014/548/oj

[3] *Amending Regulation (EU) No 548/2014 on Implementing Directive 2009/125/EC of the European Parliament and of the Council With Regard to Small, Medium and Large Power Transformers (Text With EEA Relevance)*, document 2019/1783, Commission Regulation (EU), Oct. 2019. [Online]. Available: https://eur-lex.europa.eu/eli/reg/2019/1783/oj

[4] A. Moradnouri, M. Hajiaghapour-Moghimi, and M. Vakilian, "A framework for economic and low harmonic loss distribution transformer selection based on ecodesign directive," in *Proc. Int. PSC*, 2019, pp. 19–24.

[5] E. I. Amoiralis, M. A. Tsili, and A. G. Kladas, "Power transformer economic evaluation in decentralized electricity markets," *IEEE Trans. Ind. Electron.*, vol. 59, no. 5, pp. 2329–2341, May 2012.

[6] E. I. Amoiralis, M. A. Tsili, and A. G. Kladas, "Transformer design and optimization: A literature survey," *IEEE Trans. Power Del.*, vol. 24, no. 4, pp. 1999–2024, Oct. 2009.

[7] T. Orosz, A. Sleisz, and Z. A. Tamus, "Metaheuristic optimization preliminary design process of core-form autotransformers," *IEEE Trans. Magn.*, vol. 52, no. 4, pp. 1–10, Apr. 2016.

[8] S. Maximov, M. A. Corona-Sánchez, J. C. Olivares-Galvan, E. Melgoza-Vazquez, R. Escarela-Perez, and V. M. Jimenez-Mondragon, "Mathematical calculation of stray losses in transformer tanks with a stainless steel insert," *Mathematics*, vol. 9, no. 2, p. 184, Jan. 2021.

[9] H. Wang, Q. Yang, Y. Li, and J. Wang, "Numerical analysis of the influence of magnetic shielding on stray losses and temperature rise in adjacent parts of transformer ascending flange," *IEEE Trans. Appl. Supercond.*, vol. 31, no. 8, pp. 1–4, Nov. 2021.

[10] H. Wang, Q. Yang, Y. Li, Y. Li, Y. Zhang, and J. Wang, "Numerical analysis of the effect of converter transformer combined magnetic shielding on stray load losses considering DC bias," *IEEE Trans. Appl. Supercond.*, vol. 31, no. 8, pp. 1–4, Nov. 2021.

[11] K.-H. Park, H.-J. Lee, and S.-C. Hahn, "Finite-element modeling and experimental verification of stray-loss reduction in power transformer tank with wall shunt," *IEEE Trans. Magn.*, vol. 55, no. 12, pp. 1–4, Dec. 2019.

[12] K.-H. Park, H.-M. Ahn, and S.-C. Hahn, "A study on stray loss calculation in power transformer using impedance boundary condition," in *Proc. 22nd Int. Conf. Electr. Mach. Syst. (ICEMS)*, Aug. 2019, pp. 1–5.

[13] C. Xiao, C. Dezhi, and B. Baodong, "Study of loss and temperature considering different shielding structure in power transformer," in *Proc. IEEE Int. Magn. Conf. (INTERMAG)*, Apr. 2021, pp. 1–5.

[14] C. Xiao, C. Dezhi, and B. Baodong, "Research on structure loss separation of power transformer," in *Proc. IEEE Int. Magn. Conf. (INTERMAG)*, Apr. 2021, pp. 1–5.

[15] S. Holland, G. P. O'Connell, and L. Haydock, "Calculating stray losses in power transformers using surface impedance with finite elements," *IEEE Trans. Magn.*, vol. 28, no. 2, pp. 1355–1358, Mar. 1992.

[16] W.-C. Chang and C.-C. Kuo, "A novel excitation approach for power transformer simulation based on finite element analysis," *Appl. Sci.*, vol. 11, no. 21, p. 10334, Nov. 2021.

WEN-CHING CHANG (Member, IEEE) was born in Taoyuan, Taiwan, in 1995. He received the B.S. degree in electrical engineering from the National Chin-Yi University of Technology, in 2017, and the M.S. degree in electrical engineering from the National Cheng Kung University, in 2019. He is currently pursuing the Ph.D. degree with the National Taiwan University of Science and Technology. His research interests include finite element analysis, battery storage energy systems, medium-voltage solid-state transformer, and maximum power point tracker.

CHENG-CHIEN KUO was born in Yunlin, Taiwan, in 1969. He received the B.S., M.S., and Ph.D. degrees from the National Taiwan University of Science and Technology (NTUST), in 1991, 1993, and 1998, respectively. He was with St. John's University, from 1994 to 2015. Since 2015, he has been with NTUST, where he is currently a Professor and an Assistant Head with the Department of Electrical Engineering. His research interests include fault diagnosis, conditional monitoring system design, distribution automation, partial discharge measurement, and optimization techniques.

WEN-CHENG LIN was born in Taipei, Taiwan, in 1975. He received the B.S. degree in electrical engineering from the National Sun Yat-sen University, in 1998, and the M.S. degree in electrical engineering from The University of Texas at Arlington, in 2004. He is currently a Design Engineer with the Research and Development Center, Shihlin Electric Heavy Electric Business Group, Shihlin Electric, for 18 years. He is also a Senior Project Head Supervisor, responsible for power transformer designing, finite element analysis, and power system diagnostic.

MIN-NAN HSIEH (Member, IEEE) was born in Taoyuan, Taiwan, in 1976. He received the M.S. degree in electrical engineering from Chung Yuan Christian University, in 2009. He is currently a Design Engineer with the Research and Development Center, Shihlin Electric Heavy Electric Business Group, Shihlin Electric, for 12 years. He is also responsible on the power transformer designing and finite element analysis.